

Online Detection of Sparse Changes in High-Dimensional Data Streams Using Tailored Projections

Martin Tveten and Ingrid K. Glad,
Department of Mathematics, University of Oslo

August 7, 2019

Abstract

When applying principal component analysis (PCA) for dimension reduction, the most varying projections are usually used in order to retain most of the information. For the purpose of anomaly and change detection, however, the least varying projections are often the most important ones. In this article, we present a novel method that automatically tailors the choice of projections to monitor for sparse changes in the mean and/or covariance matrix of high-dimensional data. A subset of the least varying projections is almost always selected based on a criteria of the projection's sensitivity to changes.

Our focus is on online/sequential change detection, where the aim is to detect changes as quickly as possible, while controlling false alarms at a specified level. A combination of tailored PCA and a generalized log-likelihood monitoring procedure displays high efficiency in detecting even very sparse changes in the mean, variance and correlation. We demonstrate on real data that tailored PCA monitoring is efficient for sparse change detection also when the data streams are highly auto-correlated and non-normal. Notably, error control is achieved without a large validation set, which is needed in most existing methods.

Keywords: Statistical Process Control (SPC), Principal Component Analysis, Anomaly Detection, Change-point Detection, Bootstrap/Resampling.

R packages: `tpca`, `tpcaMonitoring` and `tdpcaTEP` are available from <https://github.com/Tveten>. The packages include all code to easily reproduce our results.

Additional supplementary materials are available online (see the list at the end of the article).

1. INTRODUCTION

1.1 Motivation

The exploding availability of cheap sensors has created a need for new methods to harvest insight from them. In many applications, these sensors are deployed in large networks for online monitoring of a system. Concrete examples include temperature monitoring of a data center at Johns Hopkins (Mishin et al. 2014), plant-wide monitoring of industrial processes (Ge 2017) and semiconductor manufacturing (Zou et al. 2014). Similar technology is also used within video segmentation (Kuncheva and Faithfull 2014), solar flare detection (Liu et al. 2015), medical monitoring, DNA protein sequence analysis, network intrusion detection and speech recognition. Our own motivation comes from condition monitoring of ships, where around 100-500 sensors are placed to measure the ship’s state in terms of propulsion, temperatures, pressure and other physical quantities.

For many applications, there is a need for quick detection of anomalies that arise in the form of sustained changes in the data distribution. E.g., the pressure in a valve is too high, which should be attended to as quickly as possible, or a small number of sensors suddenly becomes faulty. This illustrates that changes may (and perhaps most often) only occur in a small subset of the sensors in an entire network. Thus, lately, several authors (see Section 1.4) have worked on the problem of change detection from the angle of only a small, unknown set of affected sensors, or so-called *sparse* changes. Mostly, they focus on changes in the mean of independent normal data, or assume all parameters in the model to be known, both before and after a change.

However, in some applications (Hawkins and Zamba 2009; Woodall and Montgomery 2014; Kuncheva and Faithfull 2014), sparse changes both in the mean and in the covariance matrix of the sensors are of interest. For instance, if a certain level of stability in a process is required, or because one has learned from historical data or experts that a group of sensors should be correlated in a specific way. Additionally, parameters are unknown in most cases and must be estimated. If estimation uncertainty is not accounted for, many false alarms will be raised, which is highly undesirable. The problem we address in this article is therefore sequential detection of sparse changes in the mean and/or covariance structure of high-dimensional data streams, with all parameters unknown. To make the method scalable, principal component analysis is incorporated and studied within this change detection framework.

1.2 Problem Formulation

Imagine a system being monitored by D sensors at times indexed by t , yielding a multivariate data stream of observations $\mathbf{x}_t \in \mathbb{R}^D$. First, there is a training period where m observations $\mathbf{x}_{-m+1}, \dots, \mathbf{x}_0$ of the system under normal conditions are generated. From $t \geq 1$ the data stream \mathbf{x}_t is monitored *online* or *sequentially* for a change in its joint distribution. The change is thought of as being a consequence of an anomaly in the system. Importantly, the anomaly might be local, and therefore only affect a small number of sensors. The aim is to detect these anomalies as soon as possible, but false alarms should be kept at a controlled level.

For simplicity, our modelling assumptions are mainly as follows, but extensions to handle time-dependency and non-normality are presented and tested in Section 5. First, there is a training period where m independent $N(\boldsymbol{\mu}_0, \boldsymbol{\Sigma}_0)$ observations \mathbf{x}_t are gathered. As monitoring ensues, observations keep arriving from the null distribution until a change-point $\kappa \geq 0$, after which the distribution of \mathbf{x}_t changes to $N(\boldsymbol{\mu}_1, \boldsymbol{\Sigma}_1)$ for all $t > \kappa$. A key element is the assumption that only a subset $\mathcal{D} \subseteq \{1, \dots, D\}$ of the sensors are affected by a change, following the perspective of Xie and Siegmund (2013). The *subset of affected streams* is defined by

$$\mathcal{D} = \{d : \mu_{0,d} \neq \mu_{1,d} \text{ or } (\boldsymbol{\Sigma}_0)_{d,*} \neq (\boldsymbol{\Sigma}_1)_{d,*}\}, \quad (1)$$

where $(A)_{d,*}$ denotes the d -th row of a matrix. In other words, we assume that the change in mean vector $\boldsymbol{\mu}_1 - \boldsymbol{\mu}_0$ and/or change in covariance matrix $\boldsymbol{\Sigma}_1 - \boldsymbol{\Sigma}_0$ has a sparsity structure. This

sparse online change-point problem is summarized by the following sequential hypothesis test:

$$\begin{aligned}
H_0 : \quad & \mathbf{x}_t \sim N(\boldsymbol{\mu}_0, \boldsymbol{\Sigma}_0), \quad t = -m + 1, -m + 2 \dots \\
H_1 : \quad & \text{There is a } \kappa \geq 0 \text{ such that} \\
& \mathbf{x}_t \sim N(\boldsymbol{\mu}_0, \boldsymbol{\Sigma}_0), \quad t = -m + 1, \dots, \kappa \\
& \mathbf{x}_t \sim N(\boldsymbol{\mu}_1, \boldsymbol{\Sigma}_1), \quad t = \kappa + 1, \kappa + 2, \dots,
\end{aligned} \tag{2}$$

where only parameters for $d \in \mathcal{D}$ change, and κ , \mathcal{D} , $\boldsymbol{\mu}_0$, $\boldsymbol{\Sigma}_0$, $\boldsymbol{\mu}_1$ and $\boldsymbol{\Sigma}_1$ are *all unknown*. Our primary interest is the high-dimensional, sparse problem, where D is high and $|\mathcal{D}|$ is relatively small. Ultimately, we end up with a stopping rule for (2) of the form

$$T = \inf\{t : \Lambda_t \geq b\}, \tag{3}$$

where Λ_t is a running test statistic of all observations, including the training set.

Note that the assumption of independence in time is less restrictive than one may think. Rather than thinking of \mathbf{x}_t as the raw observations, they can be thought of as residuals from a spatio-temporal model, learned in advance. The monitoring procedure then raises an alarm when the spatio-temporal model does not explain the incoming data well anymore.

To describe how the stopping rules T are evaluated, let \mathbb{P}^κ and \mathbb{E}^κ denote probability and expectation when there is a true change-point at κ . In particular, \mathbb{P}^∞ and \mathbb{E}^∞ mean probability and expectation under H_0 . For a chosen monitoring length n , we control the *probability of false alarms* (PFA) at a given level,

$$\mathbb{P}^\infty(T \leq n) \leq \alpha. \tag{4}$$

(This measure of false alarms compared to the more common average run length (ARL) is discussed in Section 3.) Then, if a change actually occurs at κ , the aim is to detect it as quickly as possible, measured by the (conditional) *expected detection delay* (EDD),

$$\mathbb{E}^\kappa[T - \kappa | T > \kappa]. \tag{5}$$

The EDD is the expected sample size to detect a given change. The lower it is, the better.

If one disregards the sparsity of the change, a solution to the problem (2) can be obtained through relatively straightforward generalized likelihood ratio methodology (Sullivan and Woodall 2000; Hawkins and Zamba 2009). However, these methods are not efficient in the high-dimensional and sparse change setting for several reasons. Firstly, they do not incorporate prior information about the sparsity of a change, yielding slow detection. Secondly, they scale poorly with D in terms of detection speed. To see this, let t denote the current time, $k < t$ be a candidate change-point, so that $t - k$ is the number of observations used in estimating $\boldsymbol{\Sigma}_1$. Then $t - k > D$ for a non-degenerate maximum likelihood estimate. This means that the most recent candidate change-point k will grow further apart from the current time t as D grows, resulting in very slow detection. Even if one uses regularization techniques to circumvent a singular maximum likelihood estimate, there would still be a need of an increasing amount of observations for a reliable estimate. Thirdly, they are not scalable computationally as D grows because of the burden of computing many increasingly larger covariance matrices.

Dimension reduction tools are often employed to overcome high-dimensional challenges, but they have not been studied much in the online change-point detection context. Therefore, our main objective in this work is to take a common and well understood dimension reduction tool, principal component analysis (PCA), use knowledge about how it reacts to (sparse) changes in the mean and covariance matrix, and come up with an efficient way to use it for online change detection.

Our strategy for solving the change-point problem (2) with tailored PCA is as follows:

1. Obtain the sample principal axes $\hat{\mathbf{v}}_j$, $j = 1, \dots, D$, from the training set $\mathbf{x}_{-m+1}, \dots, \mathbf{x}_0$.

(The sample principal axes are the eigenvectors of the sample covariance matrix $\hat{\Sigma}_0$.)

2. Figure out which of the projections onto sample principal axes that are most sensitive to a given set of relevant or possible changes. Pick the J most sensitive and disregard the rest.
3. For $t > 0$, monitor the mean and variance of the projections $y_{j,t} = \hat{\mathbf{v}}_j^\top \mathbf{x}_t$, $j = 1, \dots, J$. In this way, the problem of detecting changes in the entire covariance matrix is reduced to detecting changes in marginal variances.

This procedure is first studied within the modelling and evaluation framework described above to get some understanding under a clean setup, before an extension to more realistic data is proposed in Section 5.

Point (2) above is the main focus of Sections 2, while point (3) together with false alarm control is handled in Section 3. Empirical results from simulation studies are presented in Section 4. Lastly, in Section 5, our method is extended to tackle non-normal and time-dependent data, and benchmarked on the Tennessee Eastman process.

1.3 Main Contributions

There are two main contributions of this work:

1. A principled approach to automatically choosing which principal axes to keep for a specific change detection task, readily implemented in an R package. This was an open problem posed by Kuncheva and Faithfull (2014).
2. An online monitoring scheme that extends the scheme of Xie and Siegmund (2013) for sparse, positive changes in the mean of independent data, to detection of sparse changes in the mean and/or covariance matrix of time-dependent data. Our scheme is scalable, and includes all sources of estimation uncertainty when finding a threshold that meets a specified probability of false alarms, without the need of a large validation set.

Expanding on Kuncheva and Faithfull (2014) and Tveten (2019), we find that a subset of the least varying projections tend to be selected for a wide range of change scenarios and pre-change covariance matrices. We also conclude that monitoring the projections y_{jt} offer a solution to all the discussed shortcomings of a direct approach; quicker detection and computation can be attained because there are less parameters to estimate online, and information about change sparsity can be incorporated in our method for choosing projections.

1.4 Connections with Prior Work

The work in this article intersects with many fields, including anomaly and novelty detection in the machine learning world, statistical offline and online change/change-point detection, and statistical process control (SPC).

As the previous section suggests, the work in this article is mainly inspired by Xie and Siegmund (2013), Kuncheva and Faithfull (2014) and Tveten (2019). We follow Xie and Siegmund (2013) approximately in formulating the change-point problem. The difference is that they are interested in the case where the variance is known and constant, there is no correlation between the streams, and only positive changes in the mean are of interest.

On the other hand, Kuncheva and Faithfull (2014) motivated the use and study of PCA for our problem by arguing that the least varying projections were the most useful through a bivariate example. Tveten (2019) elaborate and, sometimes, correct their picture by letting the answer depend on the pre-change covariance matrix and a more comprehensive list of possible change scenarios. In contrast to Kuncheva and Faithfull (2014), Tveten (2019) traces changes that occur in the distribution of \mathbf{x}_t through the projection, and see how the distribution of the projections $y_{j,t}$ changes as a result. We build on this to develop the general method for choosing projections to monitor online for changes presented here.

The problem of sequential detection of sparse changes has received much recent interest beyond Xie and Siegmund (2013), which we have drawn upon in some way or another. Most of the research in this direction, however, is either concerned with changes in the mean of independent normals (or a known covariance matrix) (Zou et al. 2014; Wang and Mei 2015; Chan 2017), or assumes that both the pre- and post-change distributions are known (Mei 2010; Banerjee and Veeravalli 2015; Fellouris and Sokolov 2016). The work of Mei et al. (2017) is interesting and relevant in that no assumptions on the distributions are made, but it is not a fully multivariate approach.

Our motivation for the choice of performance metrics comes from discussions by Lai (1995) and Lai and Xing (2010). These works also study generalized likelihood ratio approaches where parameters have to be estimated, discuss window lengths as well as obtaining thresholds by bootstrapping. All of which is relevant to the present article.

All of the mentioned articles fall in a tradition that was initiated by Page (1955) and later expanded by Lorden (1971) and Moustakides (1986). The significant contribution of Siegmund (1985) should also be mentioned.

There is also a connection from our work to Kirch and Tadjuidje Kamgaing (2015) and Dette and Gösmann (2018), who study online change-point detection within a more recently developed theoretical framework. They consider monitoring statistics that incorporate a training set, and control the probability of false alarms under the asymptotic scheme of the number of training samples going to infinity. Their setup is very general, and contains much less rigid assumptions than the works we have mentioned so far, but does not consider sparse changes explicitly. Moreover, we control false alarms for a finite number of training samples.

Relevant literature also exists within stochastic process control. Hawkins and Zamba (2009) and Sullivan and Woodall (2000) consider the same change-point problem as in this paper, but without incorporating an assumption about the sparsity of a change. Chan and Zhang (2001) also study the detection of changes in the mean and/or covariance matrix by the use of projection pursuit as a dimension reduction tool, rather than PCA, but assume the pre-change parameters to be known. Additionally, there are plenty of control charts based on PCA (see for example the reviews Weese et al. (2015) and Rato et al. (2016)). These are, however, not set within the online change-point detection framework of controlling the false alarm rate and measuring detection delays, and they only handle sparse changes implicitly.

Within the realm of anomaly detection in machine learning, PCA has been used in numerous ways. The work in Qahtan et al. (2015) is closely related to Kuncheva and Faithfull (2014), but they use PCA in the standard way where only the most varying projections are selected. Lakhina et al. (2004) and Huang et al. (2007) use PCA to detect anomalies in (traffic) networks, and, like us, they find that it is the residual subspace of PCA that is most useful. This fact is also pointed to in the extensive review of novelty detection techniques and applications in Pimentel et al. (2014). A difference from these works to us is that what they consider as anomalies are outliers in a trained model, not changes in distribution. And, most importantly, we do not use the entire residual subspace, but rather the subspace of it that is most sensitive to a user-defined set of relevant distributional changes. Other examples of PCA-based anomaly detection procedures are Ferrer (2007), Mishin et al. (2014) and Harrou et al. (2015). None of the articles mentioned in this paragraph considers the speed of detection, which is a major difference to our objective.

2. TAILORING THE CHOICE OF PRINCIPAL AXES TO CHANGE DETECTION

In this section, the insights from Tveten (2019) about the sensitivity of projections to various changes and the dependence on the pre-change covariance matrix are knit together into an algorithm that decides which projections to use for a given change-point problem. Such an automatic choice of projections is what we mean by *tailoring* PCA for change detection. In the next section we test it in the online change detection setting.

What do we mean by sensitivity to changes? Akin to Kuncheva and Faithfull (2014) and

Tveten (2019), we define it by a divergence between the marginal distribution of each projection before and after a change. Here we follow Tveten (2019), who use the Hellinger distance. The squared Hellinger distance between two normal distributions $p(x) = N(x|\xi_1, \sigma_1)$ and $q(x) = N(x|\xi_2, \sigma_2)$ is given by

$$H^2(p, q) = 1 - \sqrt{\frac{2\sigma_1\sigma_2}{\sigma_1^2 + \sigma_2^2}} \exp\left\{-\frac{1}{4} \frac{(\xi_1 - \xi_2)^2}{\sigma_1^2 + \sigma_2^2}\right\}.$$

A desirable feature of the Hellinger distance between two normals is that it is symmetric with respect to whether the variance increases or decreases in the sense that a multiplicative increase of the variance by a factor $a \geq 1$ changes the distribution as much as a decrease by the factor $1/a$. This is also a property of the generalized likelihood ratio procedure for detecting changes in the mean and/or variance we use for monitoring later. There could be reasons for using other divergences, however, so in the accompanying R package, any divergence can be specified. Our own experiments suggest that the overall conclusions will not be significantly different by using for example the KL-divergence or Bhattacharyya distance.

Formally, the definition of sensitivity to changes we use, as defined in Tveten (2019), is as follows. Recall that $\boldsymbol{\mu}_0$ and $\boldsymbol{\Sigma}_0$ are the pre-change mean and covariance matrix of \mathbf{x}_t , while $\boldsymbol{\mu}_1$ and $\boldsymbol{\Sigma}_1$ are the post-change parameters. Without loss of generality, assume that \mathbf{x}_t is standardized with respect to the pre-change parameters, so that $\boldsymbol{\mu}_0 = \mathbf{0}$ and $\boldsymbol{\Sigma}_0$ is a correlation matrix. Next, let $\{\lambda_j, \mathbf{v}_j\}_{j=1}^D$ be the normalized eigensystem of $\boldsymbol{\Sigma}_0$, where it has been sorted such that $\lambda_1 \geq \dots \geq \lambda_D$. Then the orthogonal projections onto the pre-change principal axes are given by $y_{j,t} = \mathbf{v}_j^\top \mathbf{x}_t$, for $j = 1, \dots, D$. Assuming \mathbf{x}_t is multivariate normal, $y_{j,t}$ has marginal pre- and post-change density functions

$$\begin{aligned} p_j(y) &= N(y | \mathbf{v}_j^\top \boldsymbol{\mu}_0, \mathbf{v}_j^\top \boldsymbol{\Sigma}_0 \mathbf{v}_j) = N(y | 0, \lambda_j) \\ q_j(y) &= N(y | \mathbf{v}_j^\top \boldsymbol{\mu}_1, \mathbf{v}_j^\top \boldsymbol{\Sigma}_1 \mathbf{v}_j), \end{aligned} \tag{6}$$

respectively. Given a correlation matrix $\boldsymbol{\Sigma}_0$, the *sensitivity of the j 'th projection to the change specified by $(\boldsymbol{\mu}_1, \boldsymbol{\Sigma}_1)$* is defined as $H(p_j, q_j)$, abbreviated by H_j . Importantly, note that the sensitivity as defined here is a function of the pre- and post-change parameters of the original data \mathbf{x}_t : $\boldsymbol{\Sigma}_0$, $\boldsymbol{\mu}_1$ and $\boldsymbol{\Sigma}_1$.

Using this definition of sensitivity, Tveten (2019) proved that for bivariate normal data, the least varying projection is the most sensitive if one of the means change, one of the variances increases, or the correlation changes. If one variance decrease, then the most varying projection is the most sensitive unless the pre-change correlation is larger than $\sqrt{3}/2 \approx 0.87$. On the other hand, when both means or both variances change, there are no clear winner among the projections. Thus, we hypothesize that the least varying projections are particularly useful if changes have some sparsity structure, which they almost always are in the high-dimensional setting. The general take-away, however, is that which projections are most sensitive depends on the pre-change correlation matrix and the exact nature of the change.

The tailored PCA (TPCA) method is motivated from the bivariate results. In short, the procedure is as follows. First, an estimate of the pre-change correlation matrix, $\hat{\boldsymbol{\Sigma}}_0$, must be obtained from a training set. Then simulate B changes from a customizable *change distribution* $p(\boldsymbol{\mu}_1, \boldsymbol{\Sigma}_1 | \hat{\boldsymbol{\Sigma}}_0)$, measure each projection's sensitivity to each change, $(H_1, \dots, H_D)^{(b)}$, $b = 1, \dots, B$, and summarize the sensitivity in a way that yields a meaningful ranking of the principal axes/projections. A selection of projections can then be made from the ranking.

In principle, any distribution for $p(\boldsymbol{\mu}_1, \boldsymbol{\Sigma}_1 | \hat{\boldsymbol{\Sigma}}_0)$ could be used, but the space of all possible combinations of changes is extremely vast. Therefore, we make some restrictions to simplify the space of changes. First, we restrict ourselves to consider only one *change type* at a time. The change type can then be seen as a single-trial multinomially distributed random variable \mathbf{C} with

probabilities p_μ (mean), p_σ (variance) and p_ρ (correlation). Secondly, let $K = |\mathcal{D}| \in \{1, 2, \dots, D\}$ be the *change sparsity*, where \mathcal{D} is defined as in (1), which indicates how many dimensions that are affected by a change. I.e., the number of non-zero elements in $\boldsymbol{\mu}_1 - \boldsymbol{\mu}_0$ and $\boldsymbol{\sigma}_1 - \boldsymbol{\sigma}_0$, where $\boldsymbol{\sigma}$ is the diagonal of $\boldsymbol{\Sigma}$. For a change in correlation, a change sparsity of K means that all the correlations between the K affected dimensions change. Thirdly, given a change sparsity K , we assume throughout that the exact subset of affected streams \mathcal{D} is uniformly distributed over all combinations of size K . Fourthly, there is the *change size* of each type of change:

- $\mu_d \in \mathbb{R}$ is the size of an additive change in the mean in the d 'th component for $d \in \mathcal{D}$.
- $\sigma_d \in \mathbb{R}_{>0}$ is the size of a multiplicative change in the standard deviation in the d 'th component for $d \in \mathcal{D}$.
- a_{di} such that $a_{di}\rho_{di} \in [0, 1)$ for $d \neq i \in \mathcal{D}$ is the size of a multiplicative change in each pre-change correlation. (Not all changes of this element-wise sort will result in a positive definite correlation matrix. See the supplementary material for how we deal with this.)

Note that for practical purposes it is reasonable to restrict the domain of the change sizes to sizes that are actually relevant, but the above outlines the theoretical scope of the post-change parameter subspace we consider.

A change distribution $p(\boldsymbol{\mu}_1, \boldsymbol{\Sigma}_1 | \boldsymbol{\Sigma}_0)$ can now be characterized by a distribution over the parameters $(\mathbf{C}, K, \mathcal{D}, \mu_d, \sigma_d, a_{di})$. Due to space limitations, we will only show results for a change distribution that represents very little prior information about the nature of a change. The two minor exceptions are that we assume interest is restricted to change sparsities $K \leq D/2$ and that the correlation can only decrease. This change distribution is given by

$$\begin{aligned}
\mathbf{C} &\sim \text{Multinom}(p_\mu = 1/3, p_\sigma = 1/3, p_\rho = 1/3) \\
K &\sim \text{Unif}\{1, \dots, D/2\} \\
\mathcal{D} | K &\sim \text{Unif}\{\mathcal{D} \subseteq \{1, \dots, D\} : |\mathcal{D}| = K\} \\
\mu_d | \mathcal{D}, \mathbf{C} &\stackrel{iid}{\sim} \text{Unif}[-1.5, 1.5], \quad d \in \mathcal{D} \\
\sigma_d | \mathcal{D}, \mathbf{C} &\stackrel{iid}{\sim} \frac{1}{2} \text{Unif}[1/2.5, 1] + \frac{1}{2} \text{Unif}[1, 2.5], \quad d \in \mathcal{D} \\
a_{di} | \mathcal{D}, \mathbf{C} &\stackrel{iid}{\sim} \text{Unif}[0, 1], \quad d \neq i \in \mathcal{D}.
\end{aligned} \tag{7}$$

The supplementary material contains simulations that show that the exhibited results are fairly robust to the choice of change distribution. In the accompanying R-package `tpca`, one can easily set up uniform change distributions as in 7 over other sets of change scenarios.

By using change distribution (7) and a randomly generated 20-dimensional pre-change correlation matrix, Figure 1 illustrates that the least varying projections are the most sensitive on average, but that notable variation is hidden on the level of the exact nature of a change. To capture this variation, our idea is to estimate how often projection j is the most sensitive one for a given correlation matrix, and use this to rank the projections. That is, we want to estimate

$$P_j := \mathbb{P} \left(\underset{i \in \{1, \dots, D\}}{\text{argmax}} H(p_i, q_i) = j \mid \boldsymbol{\Sigma}_0 \right), \quad \text{for } j = 1, \dots, D. \tag{8}$$

In this way, the probability of omitting a projection that is maximally sensitive to a particular change can be controlled.

To automate the choice of a projections, a cutoff value $c \in [0, 1]$ can be selected such that the projections with the highest probability of being the most sensitive are picked until the sum of probabilities is greater than c . Then $1 - c$ corresponds to the probability of not picking a projection that is maximally sensitive to a change. Figure 2 displays the estimated probabilities

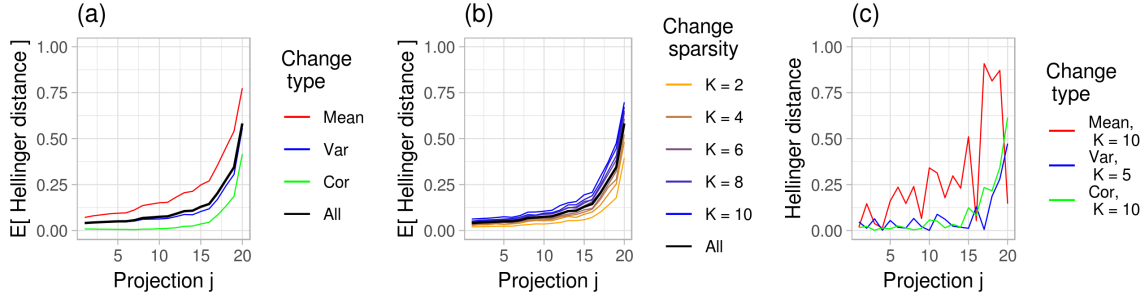


FIGURE 1. (a) and (b) display Monte Carlo estimates of $E[H_j|\Sigma_0]$, $j = 1, \dots, 20$ for a randomly generated Σ_0 , with respect to the change distribution (7). (a) show results conditional on change type and (b) on change sparsity. 10^4 Monte Carlo samples were used. Note that $j = 1$ and $j = 20$ are the most and least varying projections, respectively. (c) displays H_j for one randomly selected change in each class of change type, to illustrate what each outcome that is averaged over to obtain (a) and (b) looks like.

\hat{P}_j corresponding to the same simulations as in Figure 1. Observe that even for c close to 1, only a few of the least varying projections would be selected for all change types. However, more axes would be selected for general changes and changes in the mean than for changes in the variance or correlation. Consult the supplementary material for more simulations regarding which axes that are selected.

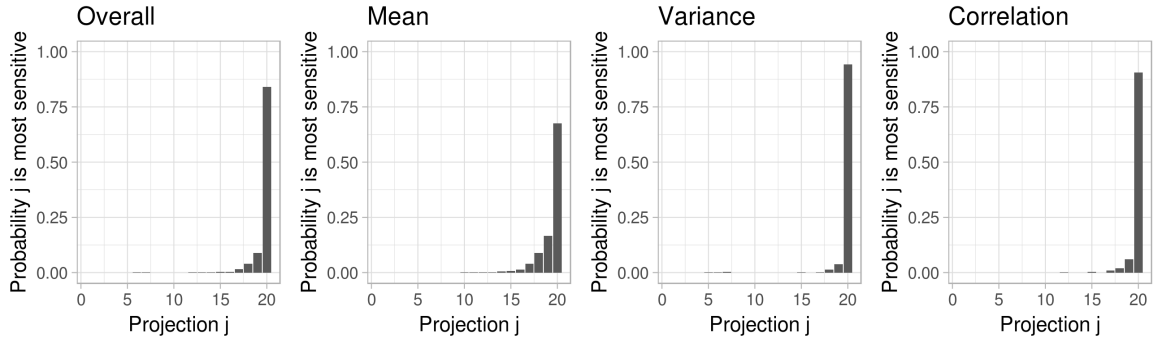


FIGURE 2. Monte Carlo estimates of P_j with respect to the same Σ_0 as in Figure 1 and same draws from change distribution (7). The three right-most figures show the contributions to the overall probabilities (left) for each change type.

To summarize, Algorithm 1 describes the tailoring procedure in detail. We call it the TPCA algorithm, and it is implemented in the R package `tpca`. For online monitoring of data streams, it is intended as a final step in the training phase. In the training phase, an estimate $\hat{\Sigma}_0$ of the pre-change correlation matrix is obtained, a change distribution $p(\mu_1, \Sigma_1|\hat{\Sigma}_0)$ is set up to represent the changes of interest, and a cutoff c is chosen. Then the tailoring algorithm is run to determine which principal axes $\mathcal{J} \in \{1, \dots, D\}$ to project the incoming data onto. Ultimately, monitoring of $\hat{\mathbf{v}}_j^T \mathbf{x}_t$, $j \in \mathcal{J}$ ensues, which we deal with next.

Algorithm 1 Tailored PCA (TPCA) for Change Detection

Input: $\Sigma_0, p(\boldsymbol{\mu}_1, \Sigma_1 | \Sigma_0), c, B$

- 1: Compute (sorted) eigenvalues and eigenvectors $\{\lambda_j, \mathbf{v}_j\}_{j=1}^D$ of Σ_0
- 2: **for** $b \in \{1, \dots, B\}$ **do**
- 3: $(\boldsymbol{\mu}_1, \Sigma_1)^{(b)} \sim p(\boldsymbol{\mu}_1, \Sigma_1 | \Sigma_0)$
- 4: $(H_1^{(b)}, \dots, H_D^{(b)}) \leftarrow (H(p_1, q_1^{(b)}), \dots, H(p_D, q_D^{(b)}))$ $\triangleright p_j$ and q_j are given in (6).
- 5: **end for**
- 6: $\hat{P}_j \leftarrow \frac{1}{B} \sum_{b=1}^B I \left\{ \operatorname{argmax}_{i \in \{1, \dots, D\}} H_i^{(b)} = j \right\}$
- 7: $\mathcal{J} \leftarrow \{j : \sum_{i \in \mathcal{J}} \hat{P}_i \geq c \text{ such that } |\mathcal{J}| \text{ is minimal}\}.$

Return: \mathcal{J} and $\{\lambda_j, \mathbf{v}_j\}_{j \in \mathcal{J}}$

3. ONLINE MONITORING

In this section, focus is shifted back to the sparse online change-point problem (2). First, the monitoring statistic we will use for performance analysis is presented, before we turn to handling the uncertainty stemming from estimating the eigensystem. We have chosen a monitoring statistic that can be set up to handle sparse changes in the mean and/or variance vectors directly in the original data \mathbf{x}_t as well as indirectly in the projections. In this way, we obtain a fair benchmark for the TPCA method, both in terms of detection speed and dimension reduction capabilities. What the monitoring statistic can not do when applied directly to the original data is to detect changes in the cross-stream correlations of \mathbf{x}_t . We view this ability as an advantage of PCA-based procedures. Whether such an ability is important or not depends on the application.

3.1 A Mixture Procedure for Detecting Changes in the Mean and/or Variance

Our monitoring statistic generalizes the mixture generalized likelihood ratio (GLR) detection procedure of Xie and Siegmund (2013) from only detecting positive mean shifts to detecting all changes in the mean and/or variance. The key component in their mixture procedure is the incorporation of a prior guess about the sparsity of the change. As before, we assume there is a training set of size m with observations from the null distribution available, and that only an unknown proportion $p = |\mathcal{D}|/D$ of the streams are affected by a change. The mixture procedure arises from the following hypothesis testing setup:

$$\begin{aligned}
 H_0 : \quad & \mathbf{x}_t \sim N(\boldsymbol{\mu}_0, \operatorname{diag}\{\boldsymbol{\sigma}_0^2\}), \quad t = -m + 1, -m + 2, \dots \\
 H_1 : \quad & \text{There is a } \kappa \geq 0 \text{ such that} \\
 & \mathbf{x}_t \sim N(\boldsymbol{\mu}_0, \operatorname{diag}\{\boldsymbol{\sigma}_0^2\}), \quad t = -m + 1, \dots, \kappa \\
 & \mathbf{x}_t \sim N(\boldsymbol{\mu}_1, \operatorname{diag}\{\boldsymbol{\sigma}_1^2\}), \quad t = \kappa + 1, \kappa + 2, \dots,
 \end{aligned} \tag{9}$$

where $\mu_{0,d} \neq \mu_{1,d}$ and/or $\sigma_{0,d}^2 \neq \sigma_{1,d}^2$ only for $d \in \mathcal{D} \subseteq \{1, \dots, D\}$. The key component in the mixture procedure of Xie and Siegmund (2013) is to substitute the unknown p with a prior guess p_0 , which acts as the probability that each stream n belongs to the class of affected streams or not. Note that it is assumed that changes occur in the mean and/or variance simultaneously, and then persist for all $t > \kappa$.

The mixture log-likelihood ratio statistic for a change in the mean and/or variance is derived in the following. With an assumed change-point at $\kappa = k \geq 0$ the global log-likelihood ratio is on the form

$$\Lambda_{k,t}(p_0) = \sum_{d=1}^D \log [1 - p_0 + p_0 \exp \{\ell_{d,k,t}\}], \tag{10}$$

where $\ell_{d,k,t}$ is the maximized likelihood ratio statistic for each stream d . So with probability $1 - p_0$ all observations in stream d are assumed to come from the same distribution, while with probability p_0 , the distribution of a stream can be different before and after k . Denote the maximum likelihood estimators for the mean and variance of each stream d by

$$\bar{x}_{d,i,l} := \frac{1}{l-i} \sum_{j=i+1}^l x_{d,j} \quad \text{and} \quad S_{d,i,l}^2 := \frac{1}{l-i} \sum_{j=i+1}^l (x_{d,j} - \bar{x}_{d,i,l})^2.$$

Then standard calculations lead us to

$$\ell_{d,k,t} = -\frac{m+k}{2} \log \frac{S_{d,-m,k}^2}{S_{d,-m,t}^2} - \frac{t-k}{2} \log \frac{S_{d,k,t}^2}{S_{d,-m,t}^2}. \quad (11)$$

See for instance Hawkins and Zamba (2005, p. 166). Note that $\Lambda_{k,t}(p_0)$ also depends on m although it is suppressed in the notation.

Ideally, a change would be declared if $\max_k \Lambda_{k,t}(p_0)$ raises above a threshold b . However, a minor correction is preferable to prevent unwanted behavior, namely, that declaration of a change is much more likely for small sample sizes $t - k$. This is so because the distribution of $\Lambda_{k,t}(p_0)$ strongly depends on the number of observations used to estimate the post-change parameters. For example, the variance of $\Lambda_{198,200}(p_0)$ is much larger than $\Lambda_{100,200}(p_0)$, making a realization from $\Lambda_{198,200}(p_0)$ more likely to be above b than $\Lambda_{100,200}(p_0)$. An often used remedy is to find a Bartlett correction (Hawkins and Zamba 2005, p. 166), where one finds a multiplicative correction factor $C(k, t)$, such that the expected value of the statistic under the null hypothesis equates to its asymptotic expected value. The asymptotic expected value of $\Lambda_{k,t}(p_0)$ under the null hypothesis is, alas, unknown. However, the asymptotic expected value of $2\ell_{d,k,t}$ is 4 due to the classical result by Wilks. Using that for a chi-square distributed X with a degrees of freedom, $\mathbb{E}[\log X] = \log 2 + \psi(a/2)$, where ψ is the digamma function, a correction factor for each stream d is given exactly by

$$\begin{aligned} \mathbb{E}[2\ell_{d,k,t}/C(k, t)] &= 4 \\ 2C(k, t) &= -(m+t) \log(m+t) + (m+t)\psi([m+t-1]/2) \\ &\quad + (m+k) \log(m+k) - (m+k)\psi([m+k-1]/2) \\ &\quad + (t-k) \log(t-k) - (t-k)\psi([t-k-1]/2). \end{aligned}$$

In total, the global corrected mixture log-likelihood ratio statistic becomes

$$\Lambda_{k,t}^C(p_0) := \sum_{d=1}^D \log [1 - p_0 + p_0 \exp \{\ell_{d,k,t}/C(k, t)\}]. \quad (12)$$

It further defines the stopping time that constitute the detection procedure,

$$T(p_0, b) := \inf \left\{ t \geq 2 : \max_{0 \leq k \leq t-2} \Lambda_{k,t}^C(p_0) \geq b \right\}. \quad (13)$$

For comparing performance, we can now apply $T(p_0, b)$ to the original data \mathbf{x}_t with various choices of p_0 , and to the projections \mathbf{y}_t with $p_0 = 1$ (since we want to see how TPCA handles sparsity on its own).

In practice, we will also restrict the set of k 's that the maximum is taken over to a set $\mathcal{K} = \{k : 2 \leq t - k \leq w + 1\}$, where w is called the *window size* and denotes the number of previous time-points that are considered as candidate change-points. This is to limit memory usage and not allow the algorithm to become slower and slower indefinitely as t grows. Choices for the set \mathcal{K} and the effect of the window size is discussed in Lai (1995). Here, we will use

$w = 200$ throughout, in line with Xie and Siegmund (2013).

3.2 Monitoring by TPCA

Algorithm 2 summarizes how TPCA is used in conjunction with the mixture monitoring procedure (13) to solve the original change-point detection problem (2). Observe that the monitored observations are the standardized projections;

$$z_{j,t} = \hat{\mathbf{v}}_j^\top \mathbf{S}_0^{-1}(\mathbf{x}_t - \hat{\boldsymbol{\mu}}_0) / \sqrt{\hat{\lambda}_j}, \quad (14)$$

for $j \in \mathcal{J}$, where $\hat{\boldsymbol{\mu}}_0$ is the training sample mean, \mathbf{S}_0 is the diagonal matrix of training sample standard deviations, and $\{\hat{\lambda}_j, \hat{\mathbf{v}}_j\}_{j \in \mathcal{J}}$ is the sample eigensystem of the training sample correlation matrix. In other words, the observations \mathbf{x}_t are first standardized by $\mathbf{u}_t = \mathbf{S}_0^{-1}(\mathbf{x}_t - \hat{\boldsymbol{\mu}}_0)$, since PCA is not invariant to scaling. These standardized observations then form the basis of PCA, and we get the projections $y_{j,t} = \hat{\mathbf{v}}_j^\top \mathbf{u}_t$. Lastly, the projections are normalized by $z_{j,t} = y_{j,t} / \sqrt{\hat{\lambda}_j}$. The reason for normalizing the projections is numerical stability, since the variance of $y_{j,t}$ for j close to D will typically be very small.

Algorithm 2 Monitoring by TPCA

Input: $b, p(\boldsymbol{\mu}_1, \boldsymbol{\Sigma}_1 | \boldsymbol{\Sigma}_0)$ and $\{\mathbf{x}_s\}_{s=-m+1}^0$.

- 1: Compute $\hat{\boldsymbol{\mu}}_0, \mathbf{S}_0$ and the correlation matrix $\hat{\boldsymbol{\Sigma}}_0$ from $\{\mathbf{x}_s\}_{s=-m+1}^0$.
- 2: \mathcal{J} and $\{\hat{\lambda}_j, \hat{\mathbf{v}}_j\}_{j \in \mathcal{J}} \leftarrow$ the results of applying Algorithm 1 to $\hat{\boldsymbol{\Sigma}}_0$ with $p(\boldsymbol{\mu}_1, \boldsymbol{\Sigma}_1 | \hat{\boldsymbol{\Sigma}}_0)$.
- 3: $z_{j,t} \leftarrow \hat{\mathbf{v}}_j^\top \mathbf{S}_0^{-1}(\mathbf{x}_t - \hat{\boldsymbol{\mu}}_0) / \sqrt{\hat{\lambda}_j}$, for $t = -m + 1, \dots, 0$ and $j \in \mathcal{J}$.
- 4: $t \leftarrow 0$ and $\Lambda_{\max,t}^C(1) = 0$.
- 5: **while** $\Lambda_{\max,t}^C(1) < b$ **do**
- 6: $t \leftarrow t + 1$ and new data \mathbf{x}_t arrives.
- 7: $\mathbf{z}_t \leftarrow (z_{j,t}) \leftarrow \hat{\mathbf{v}}_j^\top \mathbf{S}_0^{-1}(\mathbf{x}_t - \hat{\boldsymbol{\mu}}_0) / \sqrt{\hat{\lambda}_j}$ for $j \in \mathcal{J}$.
- 8: $\Lambda_{\max,t}^C(1) \leftarrow \max_{k \in \mathcal{K}} \Lambda_{k,t}^C(1)$ based on $\{\mathbf{z}_s\}_{s=-m+1}^t$.
- 9: **end while**

Return: t

It is important to note that the estimates $\hat{\boldsymbol{\mu}}_0, \mathbf{S}_0$ and $\{\hat{\lambda}_j, \hat{\mathbf{v}}_j\}_{j \in \mathcal{J}}$ are not updated as more data arrives. Ideally they would be updated for every new observation \mathbf{x}_t , but then the procedure would lose its sequential nature; all projections $z_{j,s}$ for all s would have to be recalculated at every step, as well as everything based on them. Estimating the quantities needed for the projections only once in combination with incorporating the estimation uncertainty when calibrating the threshold b is a solution that allows for both recursive computations on the projections and control of false alarms under a correctly specified model.

3.3 Controlling False Alarms

How can one set the threshold b ? As in regular hypothesis testing there is a trade-off between false positives and false negatives. There are several sequential analogs, but recall that we use the probability of false alarm (4) and the expected detection delay (5), respectively, motivated by the discussion in Lai (1995). A threshold b can now be found by choosing a segment length n and a probability of false alarm α , then solving $\alpha = \mathbb{P}^\infty[T(p_0, b) \leq n]$ for b . The EDD of the stopping rules can then be compared, where the goal is as low EDD as possible.

Remark. The *average run length* (ARL), defined as $\mathbb{E}^\infty[T(b)]$, is perhaps a more commonly used measure of false alarms. However, in many applications, a false alarm is very undesirable, and Lai (1995) argues that a more informative measure of false alarms is to consider the probability of no false alarm during a typical, steady-state period of operation. For example, an average run

length of 1000 does not necessarily mean that the probability of a false alarm during the first 100 observations is low. Another advantage is that the PFA is much more tractable to compute by Monte Carlo simulation. Finally, also pointed out by Lai (1995, p. 631), the two quantities are related approximately by

$$\mathbb{E}^\infty[T(b)] \approx n/\mathbb{P}^\infty[T(b) \leq n],$$

for the stopping rule we consider.

Finding thresholds for monitoring the raw data can be done by a relatively straight forward bootstrap procedure. Thresholds for monitoring the PCA projections, however, are slightly more complicated to attain, so this is what we focus on below. The accompanying R package `tpcaMonitoring` can be consulted for all implementational details.

Complications arise for monitoring the projections because uncertainty due to estimating the principal axes from the training data has to be incorporated. If not, there will be false alarms due to estimation error rather than an actual change in the distribution. Importantly, the estimation variance of the sample principal components can not necessarily be disregarded even for high sample sizes. This is seen from the asymptotic distribution of the eigenvectors of a sample covariance matrix $\mathbf{\Sigma}$. Recall that $\{\lambda_j, \mathbf{v}_j\}_{j=1}^d$ and $\{\hat{\lambda}_j, \hat{\mathbf{v}}_j\}_{j=1}^d$ are the population and sample eigensystems, respectively. Then $\hat{\mathbf{v}}_j$ is asymptotically multivariate normal with mean \mathbf{v}_j and covariance matrix

$$\mathbf{\Gamma}_j = \frac{\lambda_j}{n} \sum_{l \neq j} \frac{\lambda_l}{(\lambda_j - \lambda_l)^2} \mathbf{v}_j \mathbf{v}_j^\top, \quad (15)$$

given that the λ_j 's are all distinct eigenvalues (Muirhead 1982, p. 405). Hence, if there is a small gap between two population eigenvalues, the variance can be large even for large sample sizes.

The estimation uncertainty can be incorporated by the following bootstrapping procedure:

1. Input: Training data $\{\mathbf{x}_s\}_{s=-m+1}^0$ assumed to be $N(\boldsymbol{\mu}_0, \boldsymbol{\Sigma}_0)$, b , n and α .
2. Obtain estimates $\hat{\boldsymbol{\mu}}_0$ and $\hat{\boldsymbol{\Sigma}}_0$ from the training data.
3. Run the TPCA algorithm (Algorithm 1) on $\hat{\boldsymbol{\Sigma}}_0$ to get the indices $\mathcal{J} \in \{1, \dots, D\}$.
4. Draw a bootstrap training sample $\{\tilde{\mathbf{x}}_s\}_{s=-m+1}^0$, where $\tilde{\mathbf{x}}_s \stackrel{iid}{\sim} N(\hat{\boldsymbol{\mu}}_0, \hat{\boldsymbol{\Sigma}}_0)$.
5. Run Algorithm 2 on $\{\tilde{\mathbf{x}}_s\}_{s=-m+1}^0$ and equally distributed monitoring observations $\tilde{\mathbf{x}}_t \stackrel{iid}{\sim} N(\hat{\boldsymbol{\mu}}_0, \hat{\boldsymbol{\Sigma}}_0)$, $t = 1, \dots, n$. One exception is that \mathcal{J} of $\hat{\boldsymbol{\Sigma}}_0$ is reused to select projections.
6. Record $I\{T(1, b) \leq n\}$.
7. Repeat 4 - 6 B times.
8. Average the B $I\{T(1, b) \leq n\}$'s to get an estimate $\hat{\alpha}$ of $\mathbb{P}^\infty[T(1, b) \leq n]$.

Finally, repeat for different b 's until $\hat{\alpha}$ is close enough to α within a desired margin of error.

This parametric bootstrap procedure also opens the door for other ways of robustifying the threshold; pick another distribution to bootstrap training and monitoring samples from than the normal, and run the otherwise exact same simulations. For example the multivariate t -distribution or the empirical distribution function (i.e., a nonparametric bootstrap).

A drawback of using bootstrapping to get a threshold b for TPCA monitoring is that each threshold is conditional on the exact training set, which principal axes \mathcal{J} as well as the window size w . Thus, to obtain exact error control under the assumption of a correctly specified model, a new threshold must be found by simulation for every training set. Luckily, these simulations depend most strongly on the number of projections $|\mathcal{J}|$ rather than D , making it scalable. Setting up and running these simulations is the cost of incorporating all sources of uncertainty and achieving exact error control.

4. NUMERICAL PERFORMANCE ANALYSIS

In this section, the detection performance of TPCA monitoring is assessed through an extensive simulation study. The three questions we want to answer are: In terms of EDD, how well does TPCA monitoring compare to another method that also explicitly handles sparse changes? What is gained by using TPCA compared to simply picking the least varying projections? How much can the dimension be reduced by without compromising on detection speed?

4.1 Setup

In all the simulations we present here, $n = 100$ and $\alpha = 0.01$ with 95% confidence (an ARL of approximately 10^4) and $w = 200$. The main simulation study is performed for $D = 100$ and $m = 200$, while some results for $D = 500$ with $m = 1000$ are presented briefly at the end of the results section. Four different classes of methods were run on each change scenario: The mixture procedure on the raw data with method parameters $p_0 = 0.03, 0.1, 0.3, 1$, the $J = 1, 2, 3, 5, 10, 20$ most (Max PCA) and least (Min PCA) varying projections, as well as TPCA with cutoffs $c = 0.8, 0.9, 0.95, 0.99, 0.995, 0.999$. For TPCA, change distribution (7) was used with some modifications to see if incorporating information had any effect. To be precise, we assumed knowledge about which change type was of interest, so for changes in mean, for example, we set $p_\mu = 1$ and the others to 0. In addition, we set $K \leq D/2$ to emphasize sparse changes.

All the different change scenarios were considered for 30 randomly chosen pre-change correlation matrices Σ_0 , with varying strengths of correlation. For each correlation matrix, a training set of $m = 200$ observations was drawn independently from $N(\mathbf{0}, \Sigma_0)$. 15 matrices fall into a "low correlation" group and 15 into a "high correlation" group (Figure 3). "Low" and "high" refers to different choices of the α_d parameter in the method of Joe (2006) for generating random correlation matrices, where $\alpha_d < 1$ ($\alpha_d > 1$) yields a higher (lower) probability of large correlations in the space of correlation matrices. The α_d 's are evenly spread between 1 and 50 in the "low" group, while between 0.05 and 0.95 in the "high" group.

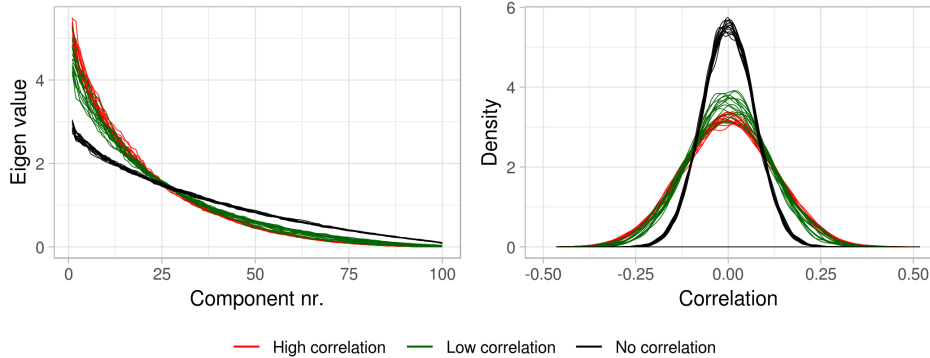


FIGURE 3. Scree plots (left) and corresponding correlation density plots (right) of the 30 random training Σ_0 's used in the simulations. As a reference for the spread of the matrices, 15 estimates based on 200 standard normal samples are also shown in black.

After a change-point at $\kappa = 0$, observations to monitor were drawn independently from $N(\mu_1, \Sigma_1)$. For all change types and sizes, the proportion of affected streams was varied over $p = |\mathcal{D}|/D = 0.02, 0.05, 0.1, 0.3, 0.5, 0.7, 0.9, 0.95, 0.98$. Which $|\mathcal{D}|$ dimensions that were changed was (uniformly) randomized in every simulated change. Considered changes in the mean were $\mu_d = 0.5, 0.7, 1, 1.3$ for $d \in \mathcal{D}$, where $\Sigma_1 = \Sigma_0$. To explain the changes in variance, note that any covariance matrix Σ can be decomposed into its variance and correlation part by $\Sigma = \mathbf{C}\mathbf{R}\mathbf{C}$, where \mathbf{R} is the correlation matrix corresponding to Σ , and \mathbf{C} is a diagonal matrix with the standard deviations σ on its diagonal. Using this relationship, keeping the mean and the correlation matrix constant, the affected standard deviation components were changed to

$\sigma_d = 0.5, 0.75, 1.5, 2$. Finally, correlations ρ_{di} were changed multiplicatively by factors $a_{di} = 0, 0.25, 0.5, 0.75$ for $d \neq i \in \mathcal{D}$, while $\boldsymbol{\mu}_1 = \boldsymbol{\mu}_0$ and $\boldsymbol{\sigma}_1 = \boldsymbol{\sigma}_0$.

In total, the setup consists of a grid of 108 change scenarios (combinations of change type, change size and change sparsity). 500 simulations of each change scenario is performed, and all the 22 combinations of methods and method parameters (p_0 , J or c) are run on every simulated data set to estimate the EDD. Finally, everything is repeated for each of the 30 training sets, including finding new thresholds for all the PCA-based method. This is important to have in mind to grasp the upcoming figures and results, which are compact summaries of a vast amount of simulations. Also note that the figures showing EDDs have $\log(p)$ on the x-axis to highlight the sparse change scenarios.

4.2 Results

When the correlations are high, monitoring the least varying projections through TPCA or Min PCA can detect almost all the tested changes immediately with an EDD of 2-3 (Figure 4 and 5, and Table 1). Particularly, even the sparsest ($p = 0.02$), smallest changes in the mean and variance ($\mu_d = 0.5$ and $\sigma_d = 0.75, 1.5$) can be detected at this speed by monitoring only the two least varying projections. I.e., a dimension reduction of 98% can be obtained, while gaining in detection speed compared to the mixture procedure. The sparsest changes in correlation is the only notable exception, where the EDD is 100-300 time-steps, depending on the size of the change. Monitoring the most varying projections leads to considerably slower detection.

TABLE 1

High correlation: Average EDD per change type for each method’s best method parameters (in parenthesis), as a summary of Figure 4. The average is taken over change sparsity, change size and the 15 full runs with different training sets. To display robustness, the listed method parameters are the ones that are within 1 time unit of the method’s minimum average EDD.

Change type	EDD			
	Max PCA(J)	Min PCA(J)	TPCA(c)	Mixture(p_0)
Mean	27.4 (20)	1.6 (2, 3, 5, 10)	1.8 (0.8, 0.9, 0.95, 0.99 0.995, 0.999)	15.2 (0.03, 0.1)
Variance	198.9 (20)	2 (2, 3, 5)	2.1 (0.8, 0.9, 0.95, 0.99 0.995, 0.999)	8 (0.03)
Correlation	50.2 (20)	10.8 (20)	22.4 (0.999)	

As the correlations between streams become smaller, the performance of the least varying projections deteriorate (Figure 6 and 5, and Table 2). In general, 10-20 projections are needed to attain a comparable performance with the mixture procedure; slightly worse performance for the denser, larger changes and better for the the sparse, small changes. Thus, when the correlations are low, some compromise on detection speed must mostly be made to reduce the dimension, but a reduction of 80 – 90% will often bring the EDD within 10 time units of the mixture procedure. The most noticeable difference from the high correlation scenario occurs when the variance decreases, where the most varying projections now are the most sensitive. Note that this behaviour is in line with the two-dimensional results of Tveten (2019, p. 5). For changes in correlation when the correlations are small, we see that an even higher c than 0.999 is needed for TPCA to pick enough axes to detect the sparse changes as efficiently as Min and Max PCA with 20 projections.

In terms of detection speed alone, there is no advantage of using TPCA compared to simply picking the axes of the least varying projections as in Min PCA; more or less the same projections are monitored under both schemes. However, Tables 1 and 2 point to the fact that TPCA will automatically choose a reasonable subset of projections quite robustly with respect to the cutoff

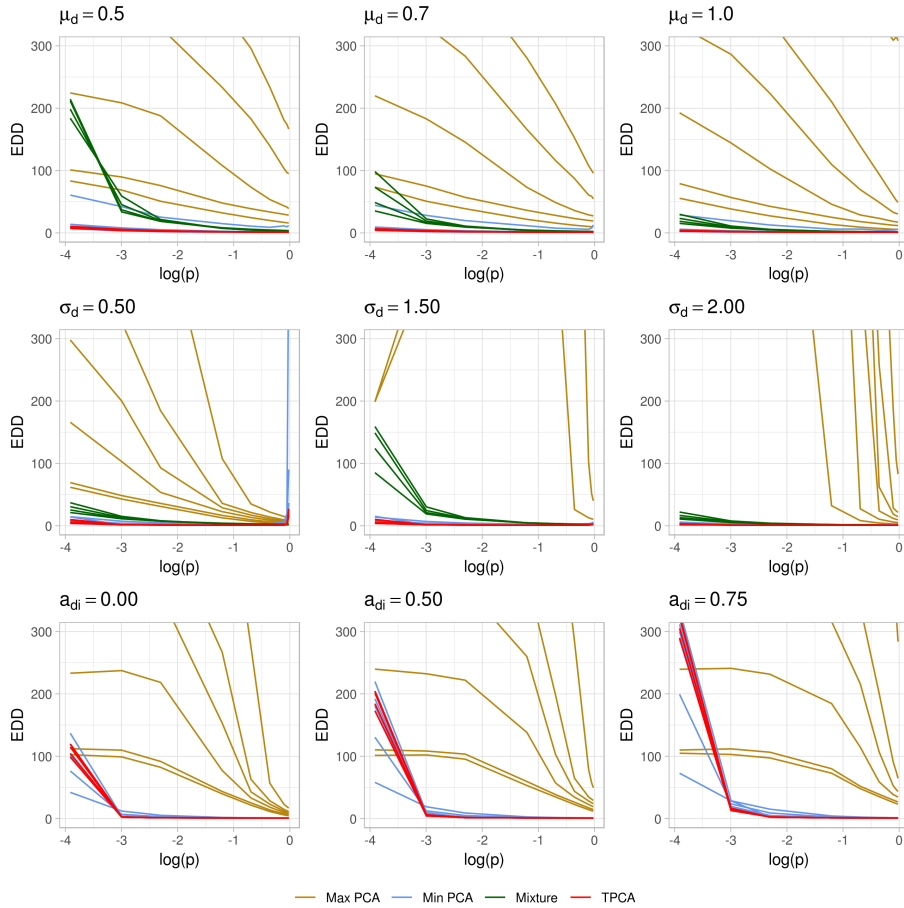


FIGURE 4. **High correlation:** EDD for changes in the mean (first row), variance (second row) and correlation (third row) of varying change sparsity and change size. Each line shows the EDD based on 500 simulations for a single method parameter, averaged over the 15 full runs with different high-correlation training sets. Note that the mixture procedure applied to the raw data can not detect changes in correlation and is thus absent from the last line of figures.

c given some knowledge about which changes are of interest. This robustness is not observed to the same degree by picking projections manually with Min PCA. The exception to this rule is for decreases in variance and changes in correlation of weakly correlated data.

Lastly, a hint towards the generalizability of these results to higher dimensions than $D = 100$ is given in Figure 7. For $D = 500$, the change sparsities tested was $p = 0.002, 0.005, 0.01, 0.02, 0.05, 0.1, 0.3$. Observe that TPCA and Min PCA are still able to detect the very sparse changes in the 500-dimensional data stream at almost the same speed as the sparse ones in the 100-dimensional stream.

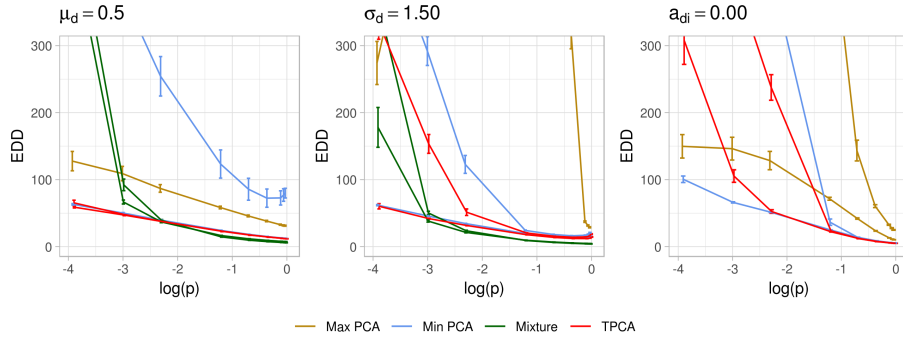


FIGURE 5. An illustration of the errors involved in Figures 4 and 6: Average EDDs with average 95% confidence intervals for a subset of method parameters. The averages are taken over all the 30 training sets, meaning that each confidence limit is an average of 30 individual limits. EDD estimates that are high or of sparse changes are generally more uncertain.

TABLE 2

Low correlation: Average EDD per change type for each method’s best method parameters (in parenthesis), as a summary of Figure 6. The average is taken over change sparsity, change size and the 15 full runs with different training sets. To display robustness, the listed method parameters are the ones that are within 1 time unit of the method’s minimum average EDD.

Change type	EDD			
	Max PCA(J)	Min PCA(J)	TPCA(c)	Mixture(p_0)
Mean	20.6 (20)	17.9 (20)	17.6 (0.9, 0.95, 0.99, 0.995, 0.999)	16 (0.03)
Variance	184.3 (20)	158.8 (10)	154.8 (0.995)	8.3 (0.03)
Correlation	30 (20)	28.5 (20)	52.3 (0.999)	

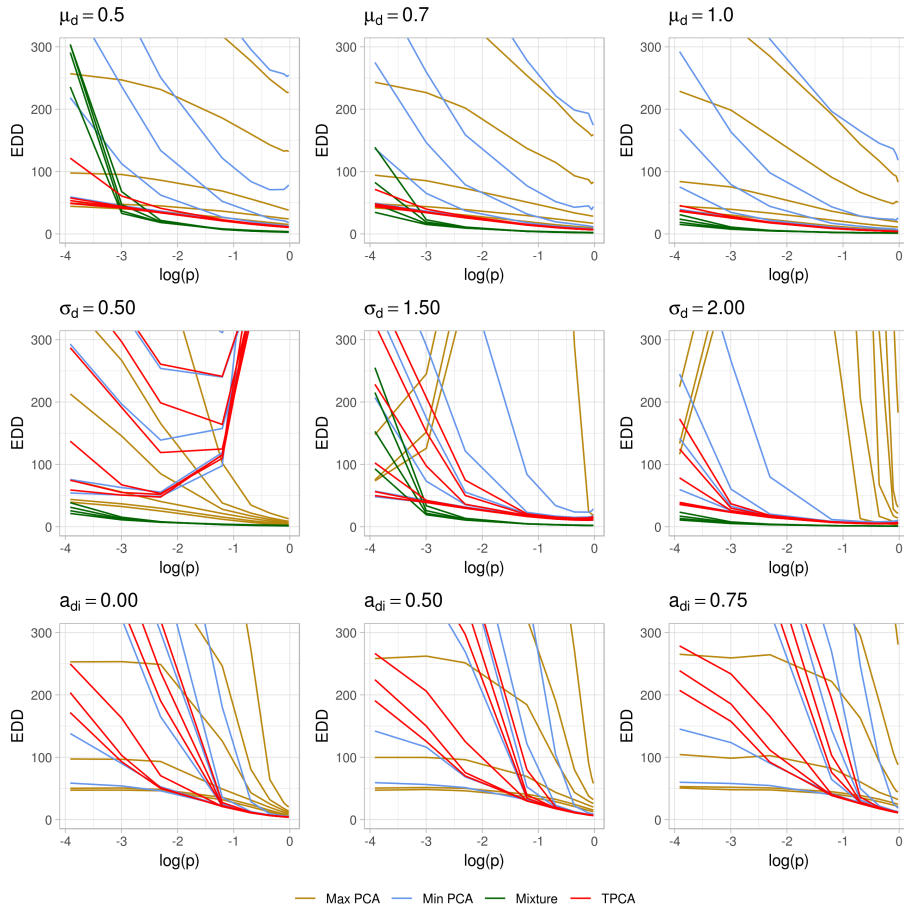


FIGURE 6. **Low correlation:** EDD for changes in the mean (first row), variance (second row) and correlation (third row) of varying change sparsity and change size. Each line shows the EDD based on 500 simulations for a single method parameter, averaged over the 15 full runs with different low-correlation training sets. Note that the mixture procedure applied to the raw data can not detect changes in correlation and is thus absent from the last line of figures.

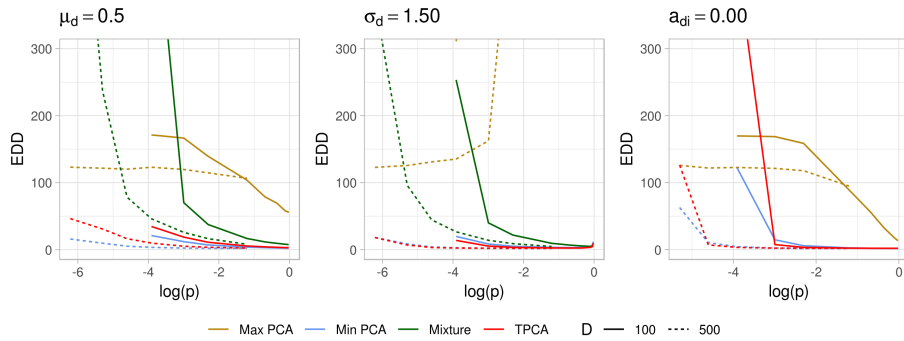


FIGURE 7. A comparison of EDDs for $D = 100, 500$ with $m = 2D$ for a single training set generated from a randomly drawn correlation matrix using $\alpha_d = 1$. Only the best choices of method parameters are shown. These figures are representative of the pattern also seen for $\mu_d = 0.7, 1$, $\sigma_d = 0.5, 2$ and $a_{di} = 0.5, 0.75$, which are omitted due to space limitations.

5. TESTING ON THE TENNESSEE EASTMAN PROCESS

In this section, TPCA is extended to handle time-dependent data and compared to dynamic PCA (DPCA) as used in the stochastic process control (SPC) literature and the method of Kuncheva and Faithfull (2014) (what we have called Min PCA or Min DPCA below). See for example Vanhatalo et al. (2017) or Rato et al. (2016) for an introduction to DPCA in SPC. The methods are tested on the well-known Tennessee Eastman Process (TEP): a model of an industrial chemical process used to generate realistic data from a large system (Downs and Vogel 1993). As a test bed, we will use the available TEP dataset from Rieth et al. (2017), which includes fault free training sets of 500 observations as well as faulty test sets of 960 observations with a change-point at $\kappa = 160$. Each observation is a sample from the process with 3 min intervals and consists of 41 direct measurements (xmeas) and 11 controlled input variables (xmv), 52 in total. There are 500 complete test sets for each of 20 different faults. Most faults cause sparse distributional changes, where faults 1-7 are changes in mean, fault 8-12 are changes in the variance, and the rest are of various other types (Rato et al. 2016). As before, we measure the EDD of detecting these faults after a short training period, now on $m = 500$ observations. We stress that this means no extra validation set is available for fine-tuning, which DPCA generally depends on.

To let TPCA account for the highly auto-correlated TEP observations, we extended it in similar fashion as PCA is extended to DPCA. I.e., a lag l is chosen, and the observation vectors \mathbf{x}_t are lag-extended to $\tilde{\mathbf{x}}_t = (\mathbf{x}_{t-l}^\top, \dots, \mathbf{x}_t^\top)^\top$ before they are fed to PCA. This induces a VAR model with lag l on the data. Then, a change distribution for \mathbf{x}_t can be set up like before, where each simulated change now corresponds to $l + 1$ duplicate changes in the parameters of $\tilde{\mathbf{x}}_t$. In this way, pre- and post-change parameters of $\tilde{\mathbf{x}}_t$ are obtained, which can be used to measure the sensitivity of the projections $\tilde{\mathbf{v}}_j^\top \tilde{\mathbf{x}}_t$, where $\tilde{\mathbf{v}}_j$, $j = 1, \dots, D(l + 1)$, are the eigenvectors of the correlation matrix of $\{\tilde{\mathbf{x}}_t\}_{t=-m+l+1}^0$. We call this method tailored dynamic PCA (TDPCA), and we will also compare it to simply picking the J most (Max DPCA) and least (Min DPCA) varying projections, like previously. It is also possible to implement a change distribution over changes in the auto-correlations, but for simplicity we keep using change-distribution (7) and close relatives. When $p_\mu = 1$, $p_\sigma = 1$ and $p_\mu = p_\sigma = p_\rho = 1/3$, we denote the methods by TDPCA(mean), TDPCA(var) and TDPCA(unif), respectively.

The main additional challenge comes from setting a valid detection threshold when the observations are not independent multivariate normal. We tackle this by switching the parametric bootstrap procedure of Section 3 with a non-parametric block bootstrap (Kunsch 1989). Thresholds are set to meet a PFA of $\alpha = 0.01$ on $n = \kappa - l$ observations with 90% confidence, for comparisons with the empirical probability of false alarms $\hat{\alpha}$.

Vanhatalo et al. (2017, p. 10) suggest lags $l = 2, 3$ or 5 for DPCA on the TE process. In our case, using lags 2 and 3 were not sufficient to capture most autocorrelation, so we proceeded with $l = 5$ for all methods as well as in the bootstrap. This yields 312-dimensional lag-extended observations with a change-point at $\kappa - l = 155$.

Before proceeding to the results, DPCA must be fit into the framework of controlling the PFA and measuring EDD. DPCA is not a change-point method, and only measures how non-conforming each new data point $\tilde{\mathbf{x}}_t$ is to the trained DPCA model by two statistics. The Hotelling's $T^2(\tilde{\mathbf{x}}_t)$ is the squared Mahalanobis distance of $\tilde{\mathbf{x}}_t$ in the DPCA model subspace, and the $Q(\tilde{\mathbf{x}}_t)$ -statistic measures the orthogonal distance of $\tilde{\mathbf{x}}_t$ to the DPCA subspace (Rato et al. 2016). The corresponding stopping rule for DPCA is $T_{\text{DPCA}} = \min(T_1, T_2)$, where

$$T_1 = \inf\{t \geq 0 : T^2(\tilde{\mathbf{x}}_t) > T_{\alpha_n}^2\} \text{ and } T_2 = \inf\{t \geq 0 : Q(\tilde{\mathbf{x}}_t) > Q_{\alpha_n}\},$$

$T_{\alpha_n}^2$ and Q_{α_n} being percentiles of each statistic's distribution. The percentiles depend on n to fulfill the PFA requirement $\mathbb{P}^\infty(T_{\text{DPCA}} \leq n) \leq \alpha$. By assuming that false alarms are equally likely for both statistics and applying a union bound, we get that $\alpha_n = \alpha/(2n)$. This is a

slightly conservative percentile. Since we do not have a validation set to find the two thresholds precisely, we use the common approximation of T^2 being χ_r^2 , where r is the number of retained components in the DPCA model, and the approximation of the Q -statistic given by Jackson and Mudholkar (1979). Since the approximation for the T^2 assumes normality and temporal independence of the retained (most varying) projections, we expect it to be overly optimistic for the TEP data, but counter-weighted somewhat by the conservative bound on α_n . Thus, it is a realistic setup in the case of no validation set, but we don't expect it to work very well in terms of false alarm control.

Lastly, in the results below, we have set the cumulative percentage of variance explained in DPCA to 95%, $J = 20$ in Min and Max DPCA, $c = 0.9$ in TPCA(mean) and TPCA(uniform), and $c = 0.99$ in TPCA(var). The reason for the cutoff-values is that these also result in approximately 20 projections being chosen, to be comparable with Min and Max PCA. Note that it is generally better to set c too high than too low, as too few projections being chosen can be detrimental, while including a few more projections than necessary only slows detection slightly. Our experiments suggest that a dimension reduction of 7 – 10% is a good choice.

The results are summarized in Table 3 and Figure 8. As expected, the proportions of false alarms for DPCA is much higher than the nominal 0.01, which disqualifies it for use in this setting. The same is the case for Max DPCA, which suffers from the most varying projections being long-range auto-correlated. Among the methods that achieve appropriate error control, one of the TDPCA variants are the quickest in all cases. In particular, note that TDPCA still beats DPCA in 13 out of 20 cases despite the considerably stricter control on false alarms. When we gave DPCA the luxury of a massive validation set to find more accurate thresholds, we still found that TDPCA beats DPCA in 15 out of 20 cases. Unexpectedly, there is no systematic relation between the type of change and whether TDPCA(mean) and TDPCA(var) is best, they are mostly almost equal, and only slightly faster than TDPCA(unif). Given the results of Section 4, it is slightly surprising that TDPCA is significantly better than Min DPCA.

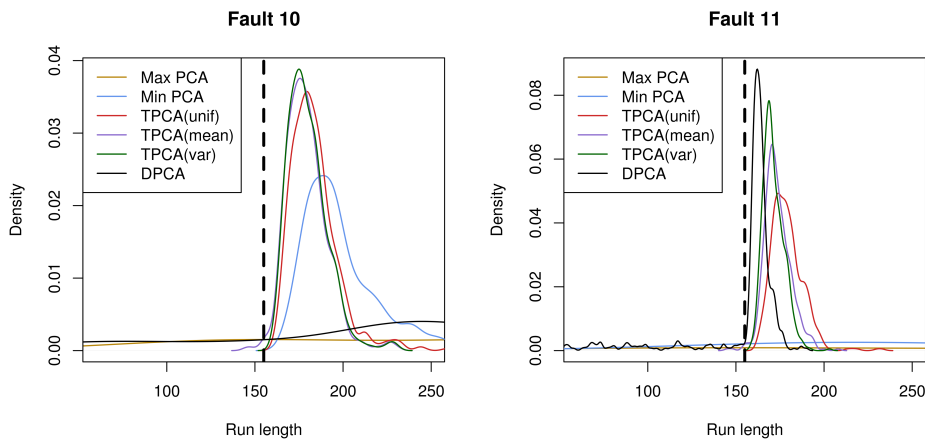


FIGURE 8. Kernel density estimates of run lengths for faults 10 and 11 of the TE process. The dashed line marks the change-point.

TABLE 3

EDD results for the TEP data. The quickest methods among those that achieve acceptable error control ($\hat{\alpha} \leq 0.01$) are in bold.

Fault	Min DPCA	TDPCA(unif)	TDPCA(var)	TDPCA(mean)	Max DPCA	DPCA
$\hat{\alpha}$	0.000	0.000	0.000	0.008	0.156	0.182
1	14.6	7.4	7.4	5.4	17.0	6.2
2	42.4	22.8	19.7	17.0	25.3	13.9
3	800.0	769.4	695.5	663.4	668.5	416.7
4	757.8	20.3	9.6	12.9	127.9	1.0
5	2.9	2.0	1.8	2.6	27.0	2.1
6	1.9	1.2	1.0	1.0	23.3	1.0
7	5.1	2.6	2.7	1.9	9.8	1.0
8	49.0	24.7	24.2	20.0	40.7	23.0
9	800.0	766.4	695.6	661.8	663.4	401.6
10	45.0	28.6	25.0	24.6	317.0	158.0
11	308.0	24.0	16.3	18.6	635.9	9.2
12	9.1	7.8	7.3	7.8	34.6	9.1
13	81.7	47.2	43.3	39.6	61.6	45.5
14	54.2	27.0	22.4	20.1	9.7	2.3
15	800.0	313.7	80.8	208.3	672.3	377.1
16	31.5	17.7	16.3	15.5	603.4	219.3
17	44.9	36.4	34.5	33.5	46.5	35.0
18	60.4	51.6	48.7	48.0	73.8	51.6
19	723.2	14.6	13.5	9.8	692.1	19.1
20	52.9	43.5	38.4	40.0	505.0	48.2

6. CONCLUDING REMARKS

The problem of detecting sparse changes in the mean and/or covariance matrix of high-dimensional data is a problem that admits no efficient direct solution because of the number of samples necessary to estimate the covariance matrix. Monitoring projections of the incoming data onto the pre-change principal axes offers an indirect solution that is also computationally scalable. Which projections to monitor for specific distributional changes is not self-evident, and this choice is what TPCA offers an answer to. We have seen that TPCA's choice of projections work well in almost all cases studied when modelling assumptions are correct, the exception being sparse changes in the correlation, and decreases in variance when the correlations are weak. Monitoring the TPCA projections work especially well if the data streams are strongly correlated, where most changes, even very sparse and small ones, can be detected almost immediately in 100-dimensional normal data. On the other hand, if correlations are weak, some performance is lost by dimension reduction, but one still gains the ability to detect changes in correlation without losing too much in detection speed for changes in the mean and variance compared to the benchmark mixture procedure.

On the TEP data, we saw that the dynamic version of TPCA combined with a non-parametric block-bootstrap procedure to robustly set thresholds worked well in detecting a wide range of changes quickly. Importantly, this was achieved without a large validation set, which is often needed to make the classic SPC tool DPCA work properly. For error control to be achieved, however, enough lags must be included so that the TDPCA projections are not subject to major auto-correlation. In terms of detection speed, TDPCA improves upon the method of Kuncheva and Faithfull (2014) (Min DPCA), and is also slightly quicker than DPCA in most cases. The superiority of TDPCA over DPCA is most notable when the changes are small and sparse,

whereas most changes in the TEP data are sparse, but large.

It should also be mentioned that we have only considered the question of when to raise an alarm. After an alarm has been raised, it is of course natural to ask which parameters and which dimensions/sensors that changed. This question is left for future research, but relevant literature already exists in e.g. Hawkins and Zamba (2009) and Lakhina et al. (2004).

Other interesting follow-up questions include: (1) How does TPCA work combined with more sophisticated tools for handling time-dependence? (2) We have studied a general pre-change covariance matrix. What if it has a known structure of a certain form, like blockwise-dependence? (3) Can the insight about PCA for change detection provided here be extended to other dimension reduction tools?

ACKNOWLEDGEMENTS

This work is partially funded by the Norwegian Research Council centre Big Insight, project 237718. We would also like to thank Kristoffer H. Hellton and Steve Marron for useful discussions regarding the theory of PCA.

SUPPLEMENTARY MATERIALS

Appendix: A) Sensitivity under other change distributions, B) Dealing with indefinite post-change correlation matrices. (.pdf document)

R-package `tpca`: The TPCA routine for selecting projections (Algorithm 1). Also includes the dynamic version of TPCA used in the TEP example. (available from <https://github.com/Tveten/tpca>)

R-package `tpcaMonitoring`: Includes an implementation of Algorithm 2 and a single function to reproduce the entire simulation study in Section 4. The package also contains .txt files with the results from our own run of the simulation study, to quickly recreate the figures. (available from <https://github.com/Tveten/tpcaMonitoring>)

R-package `tdpcaTEP`: All the code to easily reproduce the TEP results. (available from <https://github.com/Tveten/tdpcaTEP>)

REFERENCES

- Banerjee, T., and Veeravalli, V. V. (2015), “Data-Efficient Quickest Change Detection in Sensor Networks,” *IEEE Transactions on Signal Processing*, 63(14), 3727–3735.
- Chan, H. P. (2017), “Optimal sequential detection in multi-stream data,” *The Annals of Statistics*, 45(6), 2736–2763.
- Chan, L. K., and Zhang, J. (2001), “Cumulative Sum Control Charts for the Covariance Matrix,” *Statistica Sinica*, 11(3), 767–790.
- Dette, H., and Gösmann, J. (2018), “A likelihood ratio approach to sequential change point detection,” *arXiv:1802.07696 [math, stat]*, . arXiv: 1802.07696.
- Downs, J. J., and Vogel, E. F. (1993), “A plant-wide industrial process control problem,” *Computers & Chemical Engineering*, 17(3), 245–255.
- Fellouris, G., and Sokolov, G. (2016), “Second-Order Asymptotic Optimality in Multisensor Sequential Change Detection,” *IEEE Transactions on Information Theory*, 62(6), 3662–3675.
- Ferrer, A. (2007), “Multivariate Statistical Process Control Based on Principal Component Analysis (MSPC-PCA): Some Reflections and a Case Study in an Autobody Assembly Process,” *Quality Engineering*, 19(4), 311–325.

- Ge, Z. (2017), “Review on data-driven modeling and monitoring for plant-wide industrial processes,” *Chemometrics and Intelligent Laboratory Systems*, 171, 16–25.
- Harrou, F., Kadri, F., Chaabane, S., Tahon, C., and Sun, Y. (2015), “Improved principal component analysis for anomaly detection: Application to an emergency department,” *Computers & Industrial Engineering*, 88, 63–77.
- Hawkins, D. M., and Zamba, K. D. (2005), “Statistical Process Control for Shifts in Mean or Variance Using a Change-point Formulation,” *Technometrics*, 47(2), 164–173.
- Hawkins, D. M., and Zamba, K. D. (2009), “A Multivariate Change-Point Model for Change in Mean Vector and/or Covariance Structure,” *Journal of Quality Technology*, .
- Huang, L., Nguyen, X., Garofalakis, M., Jordan, M. I., Joseph, A., and Taft, N. (2007), “In-Network PCA and Anomaly Detection,” in *Advances in Neural Information Processing Systems 19*, eds. B. Schölkopf, J. C. Platt, and T. Hoffman, MA, USA: MIT Press, pp. 617–624.
- Jackson, J. E., and Mudholkar, G. S. (1979), “Control Procedures for Residuals Associated With Principal Component Analysis,” *Technometrics*, 21(3), 341–349.
- Joe, H. (2006), “Generating random correlation matrices based on partial correlations,” *Journal of Multivariate Analysis*, 97(10), 2177–2189.
- Kirch, C., and Tadjuidje Kamgaing, J. (2015), “On the use of estimating functions in monitoring time series for change points,” *Journal of Statistical Planning and Inference*, 161, 25–49.
- Kuncheva, L. I., and Faithfull, W. J. (2014), “PCA Feature Extraction for Change Detection in Multidimensional Unlabeled Data,” *IEEE Transactions on Neural Networks and Learning Systems*, 25(1), 69–80.
- Kunsch, H. R. (1989), “The Jackknife and the Bootstrap for General Stationary Observations,” *The Annals of Statistics*, 17(3), 1217–1241.
- Lai, T. L. (1995), “Sequential Change-point Detection in Quality Control and Dynamical Systems,” *Journal of the Royal Statistical Society. Series B (Methodological)*, 57(4), 613–658.
- Lai, T. L., and Xing, H. (2010), “Sequential Change-Point Detection When the Pre- and Post-Change Parameters are Unknown,” *Sequential Analysis*, 29(2), 162–175.
- Lakhina, A., Crovella, M., and Diot, C. (2004), Diagnosing Network-wide Traffic Anomalies, in *Proceedings of the 2004 Conference on Applications, Technologies, Architectures, and Protocols for Computer Communications*, SIGCOMM ’04, ACM, New York, USA, pp. 219–230.
- Liu, K., Mei, J., and Shi, J. (2015), “An Adaptive Sampling Strategy for Online High-Dimensional Process Monitoring,” *Technometrics*, .
- Lorden, G. (1971), “Procedures for Reacting to a Change in Distribution,” *The Annals of Mathematical Statistics*, 42(6), 1897–1908.
- Mei, Y. (2010), “Efficient scalable schemes for monitoring a large number of data streams,” *Biometrika*, 97(2), 419–433.
- Mei, Y., Liu, K., and Zhang, R. (2017), “Scalable SUM-Shrinkage Schemes for Distributed Monitoring Large-Scale Data Streams,” *Statistica Sinica*, .
- Mishin, D., Brantner-Magee, K., Czako, F., and Szalay, A. S. (2014), Real time change point detection by incremental PCA in large scale sensor data, in *2014 IEEE High Performance Extreme Computing Conference (HPEC)*, pp. 1–6.

- Moustakides, G. V. (1986), “Optimal Stopping Times for Detecting Changes in Distributions,” *The Annals of Statistics*, 14(4), 1379–1387.
- Muirhead, R. J. (1982), *Aspects of Multivariate Statistical Theory*, New York, USA: John Wiley & Sons.
- Page, E. S. (1955), “A test for a change in a parameter occurring at an unknown point,” *Biometrika*, 42(3/4), 523–527.
- Pimentel, M. A. F., Clifton, D. A., Clifton, L., and Tarassenko, L. (2014), “A review of novelty detection,” *Signal Processing*, 99, 215–249.
- Qahtan, A. A., Alharbi, B., Wang, S., and Zhang, X. (2015), A PCA-Based Change Detection Framework for Multidimensional Data Streams: Change Detection in Multidimensional Data Streams,, in *Proceedings of the 21th ACM SIGKDD International Conference on Knowledge Discovery and Data Mining*, KDD '15, ACM, New York, USA, pp. 935–944.
- Rato, T., Reis, M., Schmitt, E., Hubert, M., and De Ketelaere, B. (2016), “A systematic comparison of PCA-based Statistical Process Monitoring methods for high-dimensional, time-dependent Processes,” *AIChE Journal*, 62(5), 1478–1493.
- Rieth, C. A., Amsel, B. D., Tran, R., and Cook, M. B. (2017), “Additional Tennessee Eastman Process Simulation Data for Anomaly Detection Evaluation,” , . type: dataset.
- Siegmund, D. (1985), *Sequential analysis*, New York, USA: Springer.
- Sullivan, J. H., and Woodall, W. H. (2000), “Change-point detection of mean vector or covariance matrix shifts using multivariate individual observations,” *IIE Transactions*, 32(6), 537–549.
- Tveten, M. (2019), “Which principal components are most sensitive to distributional changes?” *arXiv:1905.06318 [math, stat]*, . arXiv: 1905.06318.
- Vanhatalo, E., Kulahci, M., and Bergquist, B. (2017), “On the structure of dynamic principal component analysis used in statistical process monitoring,” *Chemometrics and Intelligent Laboratory Systems*, 167, 1–11.
- Wang, Y., and Mei, Y. (2015), “Large-Scale Multi-Stream Quickest Change Detection via Shrinkage Post-Change Estimation,” *IEEE Transactions on Information Theory*, 61(12), 6926–6938.
- Weese, M., Waldyn, M., Megahead, F. M., and Jones-Farmer, L. A. (2015), “Statistical Learning Methods Applied to Process Monitoring: An Overview and Perspective,” *Journal of Quality Technology*, .
- Woodall, W. H., and Montgomery, D. C. (2014), “Some Current Directions in the Theory and Application of Statistical Process Monitoring,” *Journal of Quality Technology*, .
- Xie, Y., and Siegmund, D. (2013), “Sequential Multi-Sensor Change-Point Detection,” *The Annals of Statistics*, 41(2), 670–692.
- Zou, C., Wang, Z., Zi, X., and Jiang, W. (2014), “An Efficient Online Monitoring Method for High-Dimensional Data Streams,” *Technometrics*, .

APPENDIX A: SENSITIVITY OF PROJECTIONS UNDER OTHER CHANGE DISTRIBUTIONS

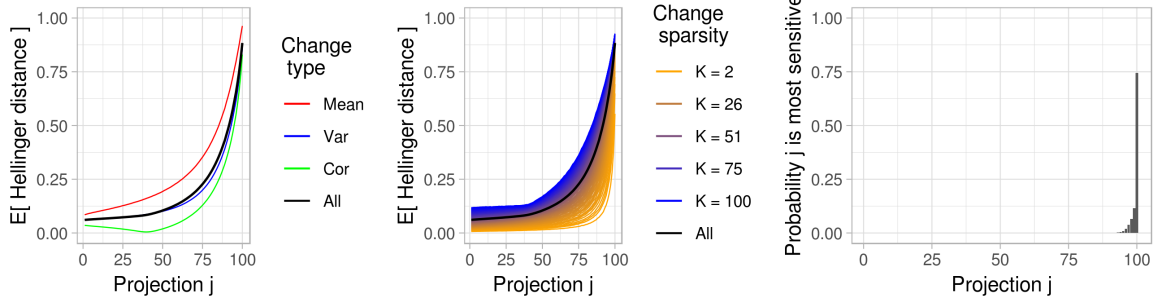


FIGURE 9. Monte Carlo estimates of $E[H_j]$ and P_j with respect to the change distribution (7) and uniformly drawn pre-change covariance matrices Σ_0 , with $D = 100$. (This is the same figures as shown in the main body of the article, for easier comparison with the figures below.) 10^3 randomly drawn Σ_0 's were used, as well as 10^3 Monte Carlo draws from the change distribution for each Σ_0

Here we present a simulation study for investigating the robustness of our results to change distribution (7), restated below for completeness.

$$\begin{aligned}
 \mathbf{C} &\sim \text{Multinom}(p_\mu = 1/3, p_\sigma = 1/3, p_p = 1/3) \\
 K &\sim \text{Unif}\{1, \dots, D/2\} \\
 \mu_d | K, \mathbf{C} &\stackrel{iid}{\sim} \text{Unif}[-1.5, 1.5], \quad d \in \mathcal{D} \\
 \sigma_d | K, \mathbf{C} &\stackrel{iid}{\sim} \frac{1}{2} \text{Unif}[1/2.5, 1] + \frac{1}{2} \text{Unif}[1, 2.5], \quad d \in \mathcal{D} \\
 a_{di} | K, \mathbf{C} &\stackrel{iid}{\sim} \text{Unif}[0, 1), \quad d \neq i \in \mathcal{D}.
 \end{aligned} \tag{7}$$

In the simulations, we set $D = 100$, and draw 10^3 Σ_0 's uniformly from the space of correlation matrices (Joe 2006). For each Σ_0 , the sensitivity to changes is assessed as in Section 2, by means of 10^3 draws from a change distribution and calculating summary statistics of the Hellinger distances. However, we now average the sensitivity results over the 10^3 Σ_0 's, to get an average picture over many pre-change conditions. Each of the figures presented below are therefore averages over 10^3 figures like the ones shown in Section 2. The average sensitivity results for change distribution (7) are shown in Figure 9.

There are four alternative change distributions we look at.

- **Larger changes:** Mean interval $[-3, 3]$, standard deviation interval $[1/4, 4]$ (with the same split between decreases and increases) and correlation interval $[0, 0.5]$.
- **Smaller changes:** Mean interval $[-0.5, 0.5]$, standard deviation interval $[1/1.5, 1.5]$ and correlation interval $[0.5, 1]$.
- **Equal changes:** The same intervals as in (7), but with all affected dimensions changing with the same value. For example, only one change size μ is drawn, and $\mu_d = \mu$ for all $d \in \mathcal{D}$.

The change parameters not mentioned have the same distribution as in (7)

Figures 10 11 and 12 show the results for the larger, smaller and equal changes, respectively. Overall, the sets of figures are very similar. If one difference is to be mentioned, it is that for cutoff values c close to 1, both the larger and smaller changes would have resulted in slightly more projections being chosen by TPCA.

Lastly, Figure 13 shows the average sensitivity results with the same change distribution (7) but now with $D = 200$,

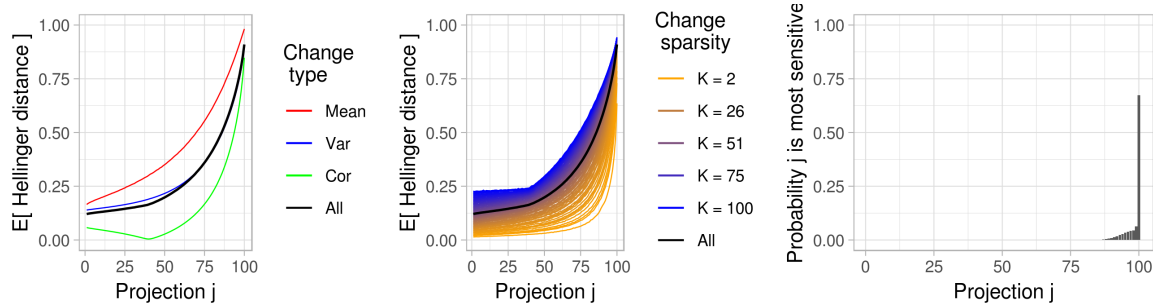


FIGURE 10. Monte Carlo estimates of $E[H_j]$ and P_j with respect to the change distribution (7) and uniformly drawn Σ_0 's, but with **larger changes**

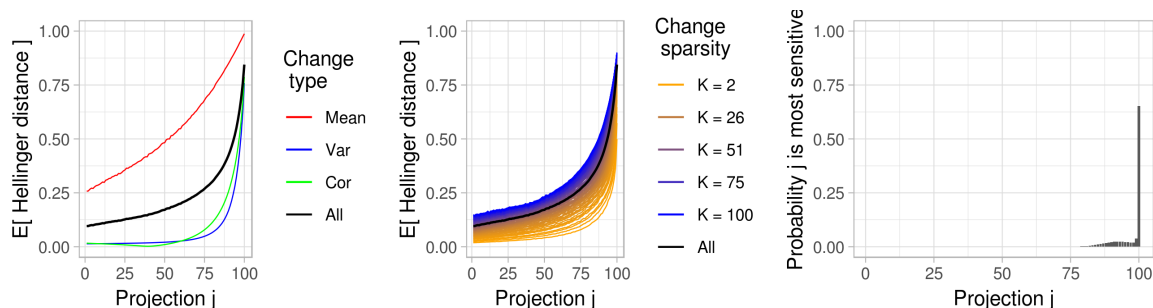


FIGURE 11. Monte Carlo estimates of $E[H_j]$ and P_j with respect to the change distribution (7) and uniformly drawn Σ_0 's, but with **smaller changes**

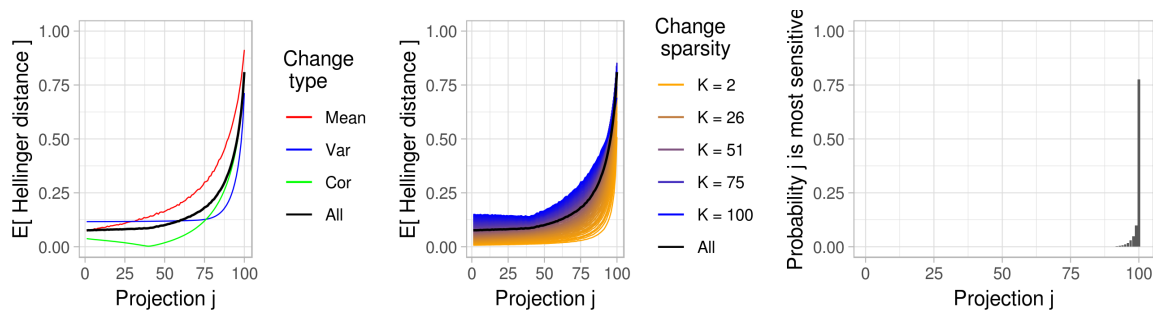


FIGURE 12. Monte Carlo estimates of $E[H_j]$ and P_j with respect to the change distribution (7) and uniformly drawn Σ_0 's, but with a **equal changes** across all affected dimensions

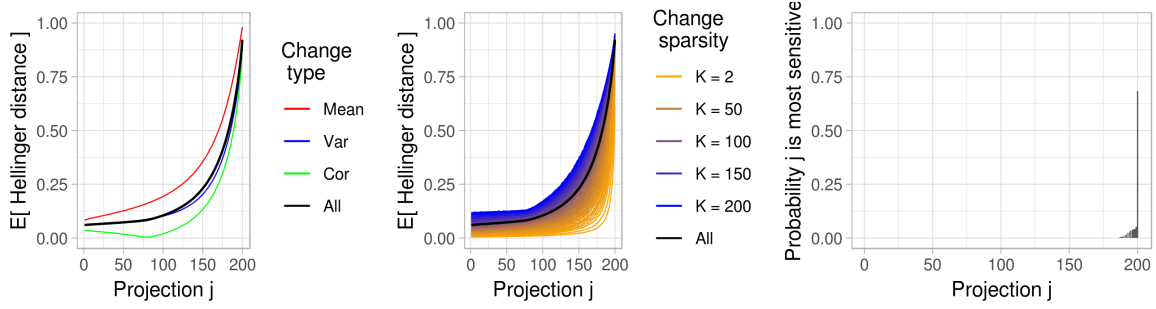


FIGURE 13. Monte Carlo estimates of $E[H_j]$ and P_j with respect to the change distribution (7) and uniformly drawn Σ_0 's, but now with $D = 200$.

APPENDIX B: DEALING WITH INDEFINITE POST-CHANGE CORRELATION MATRICES

When we change entries ρ_{di} in the correlation matrix Σ_0 by multiplying them with factors a_{di} , it is not guaranteed that the changed matrix is positive definite. To overcome this, we have used the function `nearPD` in the `Matrix` package of R. This is a function that finds the nearest positive definite matrix to the input matrix in sup norm. To obtain a correlation matrix, the diagonal is then put to 1.